6-2016

Controlled Thiol-ene Polymer Microsphere Production Using a Low-Frequency Acoustic Excitation Coaxial Flow Method

Amber D. Windham

Patrick M. Lowe

Keith W. Conley

Anton D. Netchaev

Randy K. Buchanan

See next page for additional authors

Authors

Amber D. Windham, Patrick M. Lowe, Keith W. Conley, Anton D. Netchaev, Randy K. Buchanan, and J. Paige Buchanan

Controlled Thiol-Ene Polymer Microsphere Production Using a Low-Frequency Acoustic Excitation Coaxial Flow Method

Amber D. Windham,[1] Patrick M. Lowe,[1] Keith W. Conley,[2] Anton D. Netchaev,[3] Randy K. Buchanan,[3] J. Paige Buchanan[1*]

[1] Department of Chemistry and Biochemistry, The University of Southern Mississippi, Hattiesburg, MS, 39406, United States

[2] School of Computing, The University of Southern Mississippi, Hattiesburg, MS, 39406, United States

[3] U.S. Army Engineer Research and Development Center, Information Technology Laboratory, Institute for Systems Engineering Research, 3909 Halls Ferry Road, Vicksburg, MS 39180, United States

*Address correspondence to Dr. J. Paige Buchanan, Department of Chemistry and Biochemistry, University of Southern Mississippi, 118 College Drive #5043, Hattiesburg, MS 39406; Phone: (601) 266-4083; Fax: (601) 266-6075, E-mail: paige.buchanan@usm.edu

Keywords: Thiol-ene, microspheres, acoustic disturbance

ABSTRACT

A novel technique for the production of thiol-ene microspheres using acoustic resonance and coaxial flow is reported. The method utilizes low-frequency acoustically driven mechanical perturbations to disrupt the flow of a thiol-ene liquid jet, resulting in small thiol-ene droplets that are photochemically polymerized to yield thiol-ene microspheres. Tuning of the frequency, amplitude, and monomer solution viscosity are critical parameters impacting the diameter of the microspheres produced. Characterization by optical microscopy, scanning electron microscopy, and dynamic light scattering reveal microspheres of diameters < 10 μm, with narrow particle distributions.

1. Introduction

Polymer microspheres have applications in many fields, including drug delivery,[1,2] solid phase organic synthesis,[3] solid phase extraction,[4] ion exchange,[5,6] solid supported catalysis,[7] and chromatography[8]. Several methods for the production of polymer microspheres have been published, including emulsion/suspension,[2,9] precipitation polymerization[4-6,10] microfluidics,[1,11,12] jet-break up,[13] seed polymerization,[8] and combination techniques,[14] and several excellent reviews exist.[13,15,16]

Interest in the behavior of a liquid jet and resulting formation of small droplets dates back to the work of Lord Rayleigh in 1879.[17] More recently, the widespread use of microfluidic devices in chemistry, biology, and medicine has spawned detailed reviews on the production of monodisperse droplets by investigating the behavior of two immiscible phases flowing through a microchannel.[11,18-20] Our interest lies in the development of combination techniques that utilize vibrational forces to cleave small monomer droplets. One such report came from Berkland and co-workers, who applied acoustic excitation in the kHz range (i.e. 1-70 kHz) to a nozzle delivering the discrete polymer phase which disrupted the formation of droplets at the nozzle to yield smaller diameter particles than those formed without perturbation.[1] This was paired with a flow-focusing, non-solvent carrier phase, which further decreased the droplet diameter to smaller than the nozzle opening by effectively shearing the polymer droplet away from the polymer liquid jet. Choy et al.[21] expanded on this combination by charging the polymer droplets to prevent the coalescing of droplets before hardening, further controlling diameter uniformity.

Depending on the desired application of the polymer microsphere, composition and size can vary greatly. For example, biodegradable polymers such as chitosan[2] and poly(D,L-lactide-co-glycolide) (PLG)[1], among others, are commonly used in drug delivery. Drug administration route dictates the size requirement of the microspheres, where oral administration benefits from smaller microsphere diameters (i.e., < 10 μm) while subcutaneous administration requires larger microsphere diameters (10-250 μm).[13] Studies have shown that initial drug release kinetics are controlled by the microsphere diameter, where smaller diameter microspheres release drugs faster than larger diameter microspheres.[1,22] Chromatographic applications require monodisperse microspheres giving uniform surface area throughout the entirety of the column and ensuring

optimal separation.[8,23] Subsequently, if polymer microspheres are to be loaded with markers for quantitative detection, monodisperse microspheres are necessary to ensure uniform loading.

Thiol-ene "click" chemistry was chosen as the preferred polymer matrix to investigate our novel technique, as it is a well-characterized platform and many multifunctional monomers are commercially available. The thiol-ene reaction proceeds through a free radical step-growth mechanism, yielding a highly uniform crosslinked network.[24,25] The thiol-ene reaction is readily photoinitiated which offers control of the time and placement at which the polymerization reaction occurs. Additionally, rapid rates of polymerization, insensitivity to molecular oxygen and water, and near quantitative yields are other positive attributes.[26] Others have applied thiol-ene/yne chemistry to the production of microspheres through suspension polymerization,[9,27,28] mini-emulsion,[29,30] and basic microfluidic methods.[12]

Commercially available tri-functional thiol and ene monomers were used in this study. Trimethylolpropane tris-3-mercaptopropionate (TMPMP) rapidly reacts with either pentaerythritol allyl ether (APE) or triallyl-1,3,5-triazine-2,4,6-(*1H,3H,5H*)-trione (TTT) to form highly crosslinked thiol-ene networks. The use of different monomer compositions allows for tuning of the physical properties of the networks toward specific applications, as well as a demonstration of the general nature of the synthetic method.[24,26,31] Stoichiometric adjustments of the monomer functional groups, leaving either residual C=C or SH, allows for potential surface modification to the microspheres produced, further enhancing potential utility. [28] The monomer chemical structures used in this study are provided in **Figure 1.**

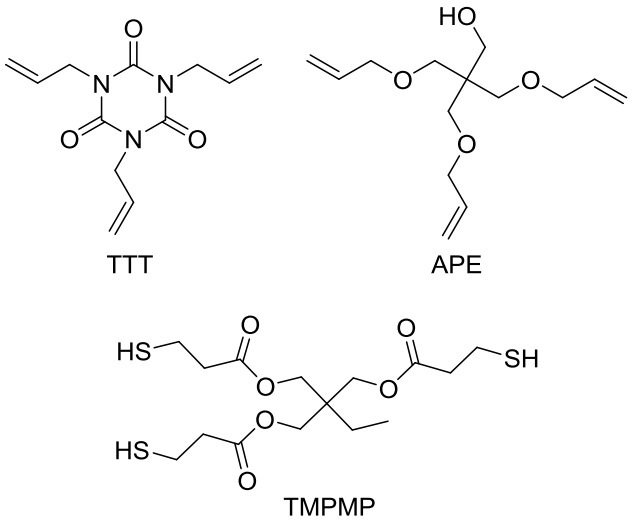

Figure 1. Chemical structures of monomers used to prepare thiol-ene microspheres: triallyl-1,3,5-triazine-2,4,6-(*1H,3H,5H*)-trione (TTT), pentaerythritol allyl ether (APE), and trimethylolpropane tris-3-mercaptopropionate (TMPMP).

Our study investigates acoustic excitation by frequencies in the low-frequency range of 50-130 Hz paired with a coaxial non-solvent carrier flow, probing other system variables such as monomer identity and viscosity. Herein, we present a continuous, scalable method for the production of thiol-ene microspheres with diameters < 10 μm, having narrow size distributions.

2. **Experimental**

2.1 Materials

Sodium dodecyl sulfate (SDS, ≥90%), pentaerythritol allyl ether (APE, 70%; remaining 30% monoene), 1,3,5-triallyl-1,3,5-triazine-2,4,6-(*1H,3H,5H*)-trione (TTT, 98%) trimethylolpropane tris-3-mercaptopropionate (TMPMP, ≥ 95%) and hexane (mixture of isomers, ≥ 98.5%) were obtained from Sigma-Aldrich. Irgacure 819 was purchased from Ciba Specialty Chemicals. Deionized water was purified using Elix® Advantage water purification system. All reagents were used as received unless noted otherwise.

2.2 AECF Apparatus and Methodology

Thiol-ene microspheres were prepared using an acoustic excitation coaxial flow (AECF) method, illustrated in Figure 2. The AECF housing is composed of acrylonitrile butadiene styrene (ABS) molded by Makerbot® Replicator® 2X 3D printer. A HiWave Classic Audio Exciter piezoelectric transducer is attached to the AECF housing and driven by an electrical excitation source. With an electric field applied across the polarized material, induced dipoles align themselves with the electric field and the transducer changes dimensions through a phenomenon known as reverse piezoelectric effect, or electrostriction. The movement of the material driven by the excitation energy produces molecular pressures at the boundary interface, thus creating wavefronts of propagating pressures at the frequency of the driven force. The AECF device is driven by a Hewlett Packard 33120A arbitrary waveform generator to allow control over parameters affecting the delivery of acoustic energy via the piezoelectric transducer driver. Delivery of the 0.5 wt % SDS non-solvent carrier phase solution to the AECF housing is performed by the Rainin Dynamax peristaltic pump through Tygon tubing (1/8 inch inner diameter) at a rate of 50 ml/min. The experimental apparatus is shown in Figure 2.

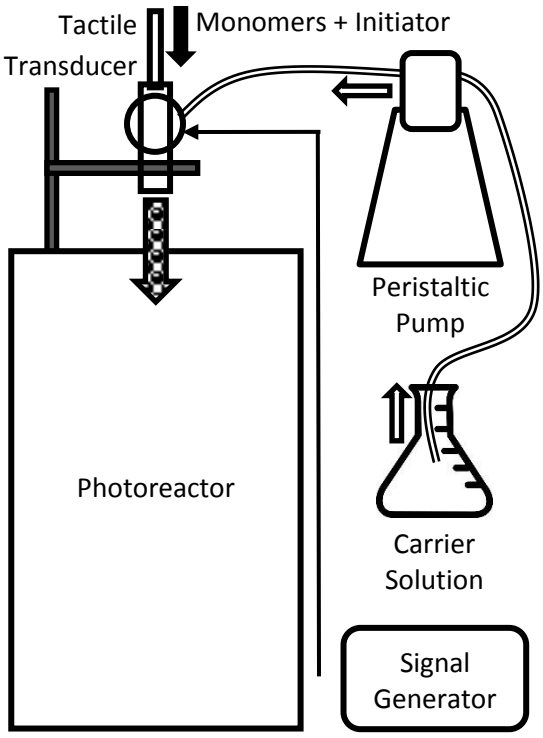

Figure 2. AECF experimental apparatus.

2.3 Preparation of Thiol-Ene Microspheres

Irgacure 819 photoinitiator (0.1 wt %) was dissolved into a tri-functional ene (APE or TTT) or ene dilution (1-10 wt % hexane) by sonication. TMPMP was then added at 1:1 thiol-ene functional group equivalence and mixed for 1 minute using a Fisher Scientific Vortex Mixer. The prepared monomer solution was immediately delivered to the apparatus through a BD Luer-Lok single-use disposable 5 ml syringe wrapped in electrical tape equipped with a BD Luer-Lok single-use 27 Gauge 1 ¼ inch needle. The suspension flows to a collection vessel with mechanical stirring inside a Rayonet Photochemical Reactor equipped with UVA lamps centered at 350 nm for photopolymerization. Thiol-ene microspheres were collected via vacuum filtration with 0.45 μm polyamide filter membrane, rinsed thoroughly with distilled water, and dried at 50 °C for 1 hour.

Filter membrane possessing dried sample appears to shimmer in light, though no MS are visible to the eye.

2.4 Characterization of AECF device

To characterize the energy profile of the AECF device, a Measurement Specialties LDT0-028K cantilevered piezoelectric transducer was attached to the AECF housing, opposite the piezo excitation driver. This transducer consisted of a piezoelectric PVDF polymer film with a 0.26 g mass near the end of the cantilever. The transducer functioned as a cantilever-beam accelerometer and was oriented in the same vibrational plane as the excitation transducer. As the transducer is displaced from its mechanical neutral axis, subsequent stressing creates very high strain within the piezopolymer and thus producing varying and measureable output voltages. The output response of the thin film provided a direct electrical/acoustical excitation energy vs. resultant mechanical oscillation correlation. Measuring the effective oscillation of the attached excitation transducer housing provided an implied correlation of oscillation in the region where droplets form at the tip of the needle, due to the rigid nature of the fixture. This disturbance was observed as a voltage output of the thin film, using the Tektronix TDS 2012B oscilloscope. Functional experimental conditions, such as similar tubing, clamping, etc., were duplicated during testing to provide measurement relevant to an actual experimental setup. A characterization of the energy profile of the AECF device was derived by applying a sine wave input with a frequency sweep from 50-170 Hz at amplitudes of 1, 2, 3, and 4 volts peak-to-peak (VPP).

2.5 Monomer and Microsphere Characterization

Viscosity of trifunctional ene monomers was investigated using a TA Instruments AR-G2 Rheometer equipped with a double walled cylinder geometry. TA instruments modulated differential scanning calorimetry (DSC) Q2000 instrument was used to determine the glass transition temperature of collected microspheres over the temperature range of -50 to 50 °C in a heat/cool/heat cycle at 5 °C/min. T_g information was obtained from the second heat cycle.

Microspheres were visualized by optical and electron microscopy. Optical microscopy (OM) images were collected using a Keyence VHX-600 digital microscope. Dry microsphere samples were collected from the filter membrane with a razor blade and placed on a clean glass microscope slide. A Zeiss Sigma VP scanning electron microscopy (SEM) was used to characterize surface features of MS. Images were obtained at 5-10 kV with 1.5-68k magnifications.

Dynamic Light Scattering (DLS) analysis was performed using a Microtrac S3500 instrumentation suite. Thiol-ene microspheres were treated as transparent spherical particles with a refractive index of 1.59. Particle sizes of the dried microspheres were collected and reported as the mean number (MN) distributions, where MN favors the size distribution of the most abundant microsphere diameter.

3. Results and discussion

The custom AECF device and instrumentation system were tailored through an iterative cycle of preliminary experiments to develop a reproducible protocol. The idealized experimental setup is described in **Figure 2**, where characterization of the device's energy profile was pursued through a systematic study of the mechanical response to low-frequency acoustic perturbation. The results of

this study were applied to the successful photochemical preparation of thiol-ene polymer microspheres.

The results of the energy profile for the AECF device are provided in Figure 3A. The study revealed that a maximum output response occurred at the applied frequency of 77 Hz for each amplitude investigated. The maximum output voltage produced by the cantilever piezo increased linearly as excitation amplitude is increased from 1 to 4 VPP, as seen in Figure 3B. The resonate frequency of the apparatus, as identified as the frequency corresponding to the maximum delivered output voltage, was essentially the same for all applied voltages.

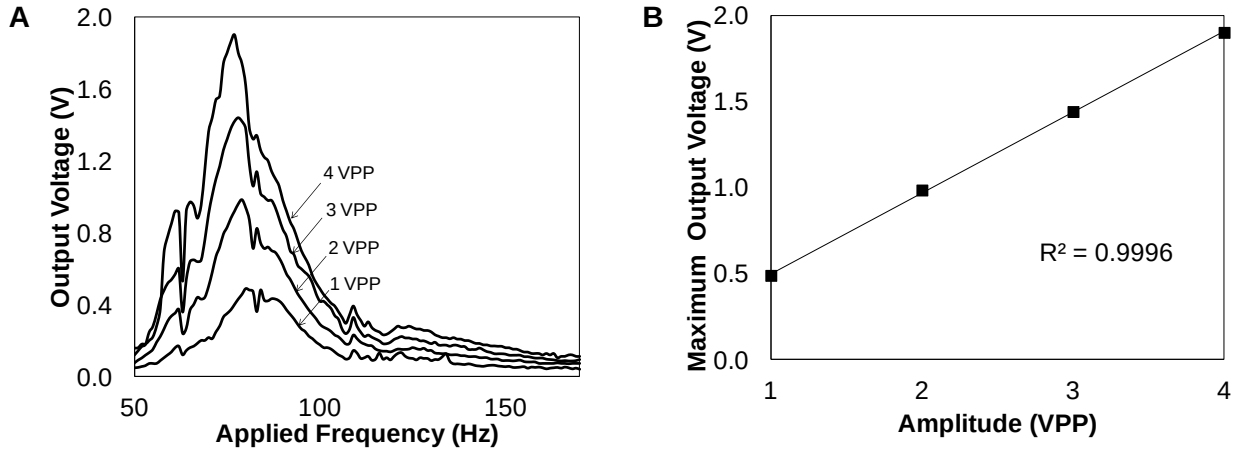

Figure 3. Results of piezoelectric evaluation of the AECF experimental apparatus: (A) output voltage measured as a result of the applied frequencies at different amplitudes, and (B) maximum output voltage measured at applied amplitudes.

Tri-functional thiol trimethylolpropane tris-3-mercaptopropionate (TMPMP) and tri-functional ene pentaerythritol allyl ether (APE) monomer combination was selected as a starting-point composition due to its rapid reaction rate and well-characterized networks. This monomer

combination has been studied extensively specifically with UV-cure conditions. [32-36] Excitation values were selected for the initial preparation of thiol-ene microspheres (Figure 3A) from the resonant frequency at 77 Hz increasing to 130 Hz. . Driving frequencies less than 77 Hz were not applied, as they were observed to negatively perturb the transducer housing and not useful for efficient bead production. APE/TMPMP microspheres were prepared at each frequency with constant amplitude (4 VPP) to analyze the influence of applied frequency on the resulting microsphere diameter. Acoustic perturbation at the applied frequencies and amplitudes was insufficient, when used alone in control experiments, to produce fully-polymerized microspheres, in the absence of photoinitiator and UV radiation. The collected microspheres were analyzed by FTIR and DSC, with both techniques supporting a high degree of polymerization. FTIR spectra show the loss of the S-H stretch at 2565 cm^{-1} and C=C-H stretch at 3080 cm^{-1} upon polymerization, **Figure S1**. Through DSC analysis, microspheres were determined to have glass transition temperatures characteristic of the bulk materials (**Figure S2)**.[33,35] Particle size was monitored using DLS. Multiple batch experiments were performed at each frequency, and the range of diameters obtained from each frequency set (≥ 3 trials) are summarized in **Table 1**. For example in the 77Hz data set, the individual batch experiments yielded average diameters of 3.4, 3.6, and 4.1 μm, with standard deviations as low as 3-4%. Within a given collection, there is a high degree of reproducibility at this frequency, although there is some variation in the average diameter from run to run.

Table 1. DLS results of APE/TMPMP samples prepared at a constant amplitude varying applied frequency

Frequency (Hz) at 4VPP amplitude	MN (μm) [a]
77	3.4 – 4.1
80	4.1 – 183
90	2.1 – 3.8

100	2.5 – 118
130	3.7 – 13.5

[a] Mean number range obtained from ≥ 3 trials, lowest to highest average diameter

Notably, two experimental frequencies, 77 Hz and 90 Hz produced highly uniform microspheres in the 2-4 μm range. However, low yields were obtained from experiments performed at off-resonant frequencies, making characterization of the microspheres difficult. Therefore, off-resonant experimental conditions were not pursued for the remainder of the study. Characterization by OM was performed to support the data obtained by DLS. For microspheres prepared at 77 Hz, images were obtained by OM and SEM (**Figure 4.1D**). A high population of uniform particles < 10 μm are visible in OM images, and a magnified image obtained by SEM reveals microspheres with a smooth surface and diameter of ≈ 4 μm. This corresponds closely with the diameter range obtained by DLS (**Table 1**). OM images of microspheres prepared at 80 and 100 Hz (provided in supplemental, **Figure S3**) are consistent with the wide range of diameters suggested by DLS. These results supported that the applied excitation energy of 77 Hz was optimum to produce microspheres with the most consistent diameter. The resonant frequency may be credited to the maximal disturbance and high levels of shear forces at the site of droplet formation, resulting in smaller, more uniform thiol-ene microspheres. Off-resonant frequencies were observed to deliver less uniform energy to the site of droplet formation, thus yielding microspheres with increased polydispersity of diameters and low yields.

The role of the magnitude of applied excitation energy in the production of APE/TMPMP MS by AECF was also investigated. Using an excitation frequency of 77 Hz, microspheres were prepared at amplitudes 1, 2, and 3 VPP for comparison to the previously prepared 77 Hz 4 VPP samples. **Table 2** lists the results according to DLS. **Figure 5.1A-1D** shows OM images, which are consistent with DLS data. Microspheres prepared at 2 VPP and 3 VPP show a wider range of

particle sizes than those prepared at 1 VPP and 4 VPP. SEM images (**Figure 5.2A-2D**) provide a closer look at individual microspheres. In the case of 3 VPP microspheres shown in **Figure 5.2C**, aggregation of microspheres is apparent. While all experimental settings produced microspheres with very similar diameters, the largest excitation amplitude of 4VPP offered the smallest standard deviation by DLS and good uniformity throughout the sample, as seen in OM. This could be attributed to a higher amplitude of produced acoustic energy affecting a greater disturbance and subsequently a greater influence during the formation of the droplet at the tip of the needle, thus producing microspheres with a more controlled diameter range.

Table 2. DLS results of APE/TMPMP samples prepared at a constant applied frequency varying wave amplitude.

Amplitude (VPP) at 77 Hz	MN (μm)[a]	SD (μm)
1	3.8	±1.0
2	4.7	±3.4
3	4.4	±1.4
4	3.7	±0.41

[a] Mean number average based on 3 trials.

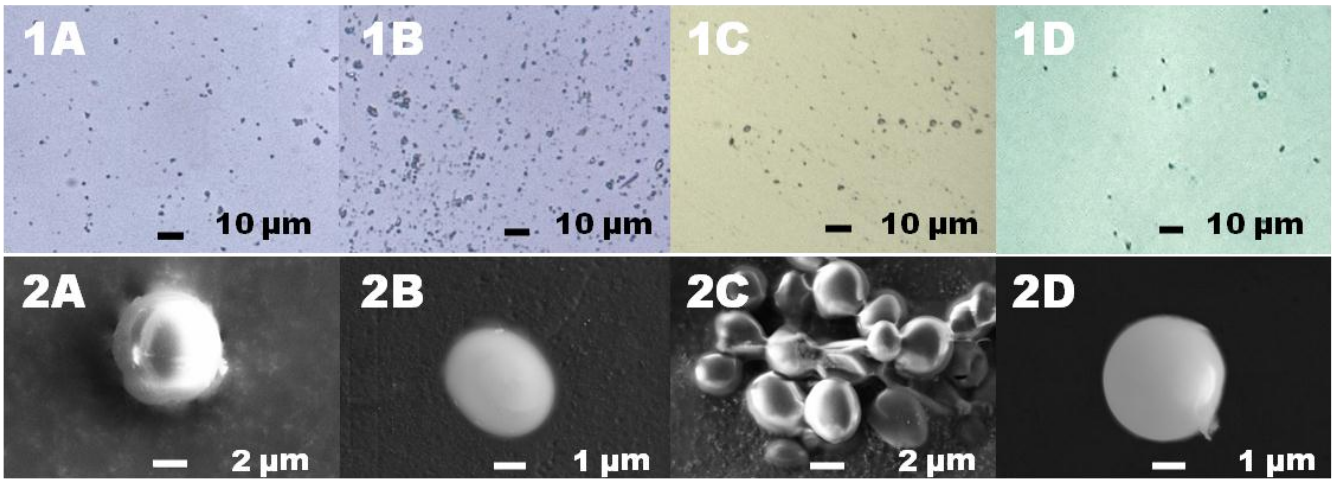

Figure 4. Images of APE/TMPMP microspheres produced at varied amplitude. Row 1: Optical microscope images, collected at 1000x magnification, at (A) 1, (B) 2, (C) 3, and (D) 4 VPP, where scale bars are 10 µm. Row 2: SEM images at (A) 1, (B) 2, (C) 3, and (D) 4 VPP, at various magnifications, where scale bars are noted.

An additional series of samples was prepared using the APE/TMPMP monomer composition at the frequencies that produced maximum output response, for further examination of frequency to microsphere diameter correlations. Results are detailed in **Table 3.** As anticipated, insignificant deviation in microsphere dimensions was observed over the small range in peak frequencies.

Table 3. Results of varying frequency on APE/TMPMP microspheres.

VPP	Frequency (Hz)	MN (µm)	SD (µm)
1	80	3.3	±1.0
2	79	3.7	±0.87
3	78	2.9	±0.92
4	77	3.7	±0.41

Having determined optimal settings for microsphere production, the ability to translate this platform to a 2nd monomer composition was explored using trifunctional ene TTT with TMPMP, a combination that has also been well- characterized.[33,36,37] Ene and thiol were maintained at 1:1

reactive group equivalence. The flow of the monomer mixture through the AECF apparatus was significantly reduced, resulting in very low yields of microspheres, making characterization of this composition difficult. Investigation of viscosities by TA Instruments AR-G2 Rheometer revealed a value of 14.2 cP (21 °C) for TTT, significantly higher than the 4.61 cP (21 °C) for APE. To address the phenomenon, a series of TTT ene dilutions were prepared by the addition of hexane as a diluent to TTT before combining with TMPMP and photoinitiator. This mixture was used in the preparation of microspheres following standard reaction conditions. **Table 4** outlines the composition and DLS results of the microspheres prepared in the dilution series. TTT/TMPMP microspheres displayed decreasing diameters with increased hexane content, with the smallest MN of 0.66 μm.

Table 4. Compositions of MS prepared with TMPMP and TTT diluted with hexane and corresponding mean number (MN) values obtained by DLS.

Sample ID	Wt% hexane in TTT	MN (μm)	SD (μm)
0%	0	*	*
1%	1	4.9	1.7
2.5%	2.5	4.3	1.6
5%	5	3.5	0.66
7.5%	7.5	3.1	0.46
10%	10	0.66	0.087

*Insufficient sample

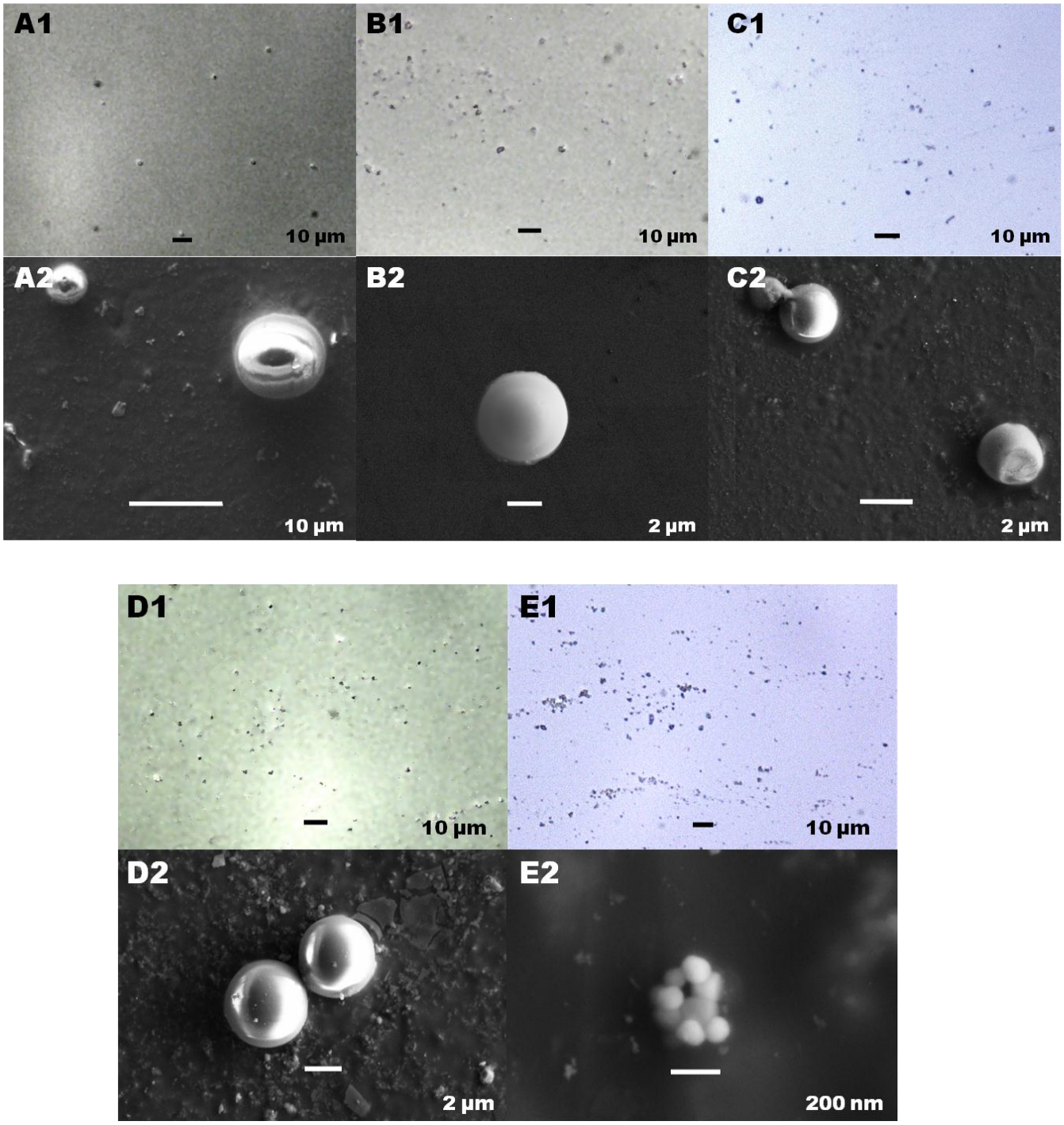

Figure 5. Images of TTT/TMPMP dilution series prepared at 77Hz 4VPP, where optical images are in Row 1, with ene dilutions of (A) 1, (B) 2.5, (C) 5, (D) 7.5, & (E) 10.0 wt% hexane. SEM images are in Row 2, with ene dilutions corresponding to Row 1. Scale bars are noted.

Polymer microsphere average diameters were supported by OM and SEM images, shown in **Figure 5**. An obvious consequence that occurred with increasing dilution is the increased yield of microspheres collected (**Figures 5.1A-E**). SEM micrographs provide a closer look at the microspheres, allowing estimation of diameter. The SEM images are in agreement with DLS information, confirming that increasing the amount of hexane in ene does produce smaller microspheres. However, no obvious change in microsphere porosity was observed as a result of the added hexane. For **Figure 5 E1&2**, OM shows what appears to be larger microspheres of ≈ 5 μm, but SEM reveals significantly smaller microspheres that are clustered together. Comparing this to the DLS MN of 0.66 μm, the clusters are on the same order of magnitude.

Additionally, the effect of the continuous phase flow rate on the microsphere diameter was investigated. For all previous studies, a rate of 50 mL/min was used for the aqueous continuous phase. Flow rates ranging from 25 ml/min to 100 ml/min were tested with constant frequency (77 Hz) and amplitude (4 VPP). Results on the dependence of microsphere size with continuous phase flow rate are summarized in **Table 5**. As the flow rate was increased, a decrease in microsphere diameter was observed in conjunction with a narrowing of the standard deviation. This data supports that control over continuous flow rate offers additional influence on the size and size distribution of the microspheres produced.

Table 5. Results of the continuous flow rate on microsphere diameter using 1% hexane TTT/TMPMP with applied frequency of 77 Hz and amplitude of 4 VPP.

Flow rate	MN (μm)	SD (μm)
25 mL/min	5.2	±2.2
50 mL/min	4.9	±1.7
80 mL/min	3.0	±0.75
100 mL/min	2.9	±0.93

4. Conclusion

Acoustic excitation coaxial-flow method for the production of thiol-ene microspheres has been investigated with the production of uniform microspheres from two thiol-ene monomer compositions. This method offered customization of several variables used in the preparation of microspheres of a narrow size distribution ranging from 400 nm to 5 μm as determined by DLS and microscopy techniques. Application of excitation energy to the syringe through the AECF device offered generation of smaller than syringe diameter microspheres, as well as control of the size distribution. Additionally, applying a greater amplitude of excitation energy for the generation of acoustic waves at resonance within the linear range of maximum perturbation offered experimental results with higher monodispersity. Decreasing solution viscosity was shown to decrease the microsphere diameter and increase the batch yield. Finally, the rate of the continuous flow phase was shown to offer additional control over the microsphere diameter range and standard deviation. Overall, this technique is a useful, scalable method for the production of monodisperse microspheres for a variety of applications.

Acknowledgement

Special thanks to Jessica Douglas for SEM imaging. Financial support for this work was provided through the National Science Foundation CAREER Program Award CHE-0847481 and the NSF GK-12 Program-University of Southern Mississippi, "Connections in the Classroom: Molecules to Muscles" Award 0947944.

References

(1) Berkland, C.; Kim, K. K.; Pack, D. W. *Journal of Controlled Release* **2001**, *73*, 59-74.

(2) Dave, K.; Purohit, S. *International Journal of Pharma and Bio Sciences* **2013**, *4*, 402-415.

(3) Lumpi, D.; Braunshier, C.; Horkel, E.; Hametner, C.; Frohlich, J. *ACS Combinatorial Science* **2014**, *16*, 367-374.
(4) Wu, X.; Liang, S.; Ge, X.; Lv, Y.; Sun, H. *Journal of Separation Science* **2015**, *38*, 1263-1270.
(5) Cormack, P. A. G.; Davies, A.; Fontanals, N. *Reactive and Functional Polymers Special Issue in Honour of Prof. David C. Sherrington FRS. Functional polymers between chemistry and applications* **2012**, *72*, 939-946.
(6) Bratkowska, D.; Davies, A.; Fontanals, N.; Cormack, P. A. G.; Borrull, F.; Sherrington, D. C.; Marce, R. M. *Journal of Separation Science* **2012**, *35*, 2621-2628.
(7) Quaranta, E.; Angelini, A.; Carafa, M.; Dibenedetto, A.; Mele, V. *ACS Catalysis* **2014**, *4*, 195-202.
(8) Haginaka, J. *Journal of Chromatography B: 50 Years Journal of Chromatography* **2008**, *866*, 3-13.
(9) Durham, O. Z.; Krishnan, S.; Shipp, D. A. *ACS Macro Letters* **2012**, *1*, 1134-1137.
(10) Li, G. L.; Moehwald, H.; Shchukin, D. G. *Chemical Society Reviews* **2013**, *42*, 3628-3646.
(11) Serra, C. A.; Chang, Z. *Chem. Eng. Technol.* **2008**, *31*, 1099-1115.
(12) Prasath, R. A.; Gokmen, M. T.; Espeel, P.; Prez, F. E. D. *Polymer Chemistry* **2010**, *1*, 685-692.
(13) Tran, V.-T.; Benoit, J.-P.; Venier-Julienne, M.-C. *Int. J. Pharm.* **2011**, *407*, 1-11.
(14) Kim, K. K.; Pack, D. W. In *Biological and Biomedical Nanotechnology*; Lee, J., Ed.; Springer, 2006; Vol. I, pp 19-50.
(15) Gokmen, M. T.; Brassinne, J.; Prasath, R. A.; Du Prez, F. E. *Chemical Communications* **2011**, *47*, 4652-4654.
(16) Dowding, P. J.; Vincent, B. *Colloids and Surfaces A: Physicochemical and Engineering Aspects* **2000**, *161*, 259-269.
(17) Rayleigh, L. *Proceedings of the Royal Society of London* **1879**, *29*, 71- 97.
(18) Nunes, J. K.; Tsai, S. S. H.; Wan, J.; Stone, H. A. *Journal of Physics D: Applied Physics* **2013**, *46*, 114002.
(19) Utada, A. S.; Chu, L.-Y.; Fernandez-Nieves, A.; Link, D. R.; Holtz, C.; Weitz, D. A. *MRS Bulletin* **2007**, *32*, pp 702-708.
(20) Guillot, P.; Colin, A.; Ajdari, A. *Physical Review E* **2008**, *78*, 013607.
(21) Choy, Y. B.; Choi, H.; Kim, K. *Macromolecular Bioscience* **2007**, *7*, 423-428.
(22) Berkland, C.; Kim, K. K.; Pack, D. *Pharmaceutical Research* **2003**, *20*, 1055-1062.
(23) Benes, M. J.; Horak, D.; Svec, F. *Journal of Separation Science* **2005**, *28*, 1855-1875.
(24) Hoyle, C. E.; Lee, T. Y.; Roper, T. *Journal of Polymer Science: Part A: Polymer Chemistry* **2004**, *42*, 5301-5338.
(25) Lowe, A. B. *Polymer Chemistry* **2010**, *1*, 17-36.
(26) Hoyle, C. E.; Bowman, C. N. *Angewandte Chemie* **2010**, *49*, 1540-1573.
(27) Durham, O. Z.; Shipp, D. A. *Polymer* **2014**, *55*, 1674-1680.
(28) Durham, O. Z.; Norton, H. R.; Shipp, D. A. *RSC Advances* **2015**, *5*, 66757-66766.
(29) Amato, D. V.; Amato, D. N.; Flynt, A. S.; Patton, D. L. *Polymer Chemistry* **2015**, *6*, 5625-5632.
(30) Amato, D. N.; Amato, D. V.; Narayanan, J.; Donovan, B. R.; Douglas, J. R.; Walley, S. E.; Flynt, A. S.; Patton, D. L. *Chemical Communications* **2015**, *51*, 10910-10913.

(31) Hoyle, C. E.; Lowe, A. B.; Bowman, C. N. *Chemical Society Reviews* **2010**, *39*, 1355-1387.

(32) Clark, T.; Kwisnek, L.; Hoyle, C. E.; Nazarenko, S. *J. Polym. Sci. A Polym. Chem.* **2009**, *47*, 14-24.

(33) Shin, J.; Nazarenko, S.; Hoyle, C. E. *Macromolecules* **2008**, *41*, 6741-6746.

(34) White, T. J.; Natarajan, L. V.; Tondiglia, V. P.; Bunning, T. J.; Guymon, C. A. *Macromolecules* **2007**, *40*, 1112-1120.

(35) Phillips, J. P.; Mackey, N. M.; Confait, B. S.; Heaps, D. T.; Deng, X.; Todd, M. L.; Stevenson, S.; Zhou, H.; Hoyle, C. E. *Chemistry of Materials* **2008**, *20*, 5240-5245.

(36) Jefferson, L. U.; Netchaev, A. D.; Jefcoat, J. A.; Windham, A. D.; McFarland, F. M.; Guo, S.; Buchanan, R. K.; Buchanan, J. P. *ACS Applied Materials & Interfaces* **2015**, *7*, 12639-12648.

(37) Zhou, H.; Li, Q.; Shin, J.; Hoyle, C. E. *Macromolecules* **2009**, *42*, 2994-2999.

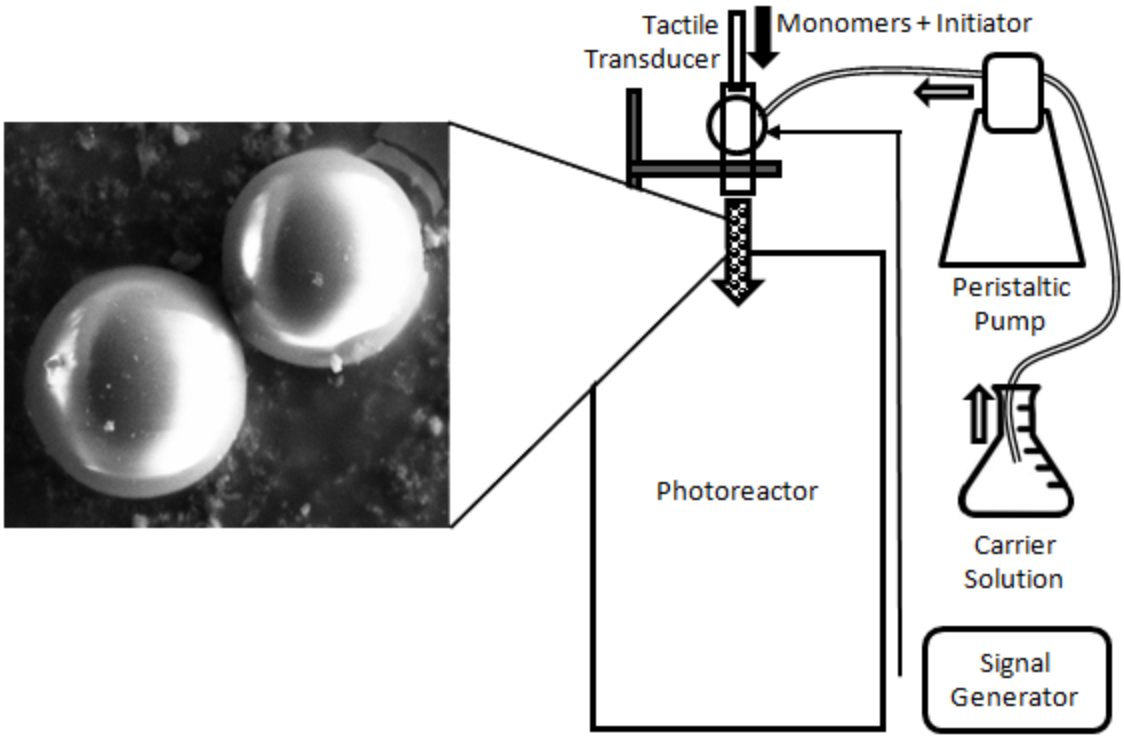
Tactile
Transducer
Monomers + Initiator
Peristaltic
Pump
Photoreactor
Carrier
Solution
Signal
Generator